

Mixed Chloride/Azide Complexes of Arsenic and Antimony

Thomas M. Klapötke,^{*,[a]} Heinrich Nöth,^{[a],[‡]} Thomas Schütt,^[a] and Max Suter^{[a],[‡]}

Keywords: Azides / Antimony / Arsenic / Lewis acids / Lewis bases / Density functional calculations

The Lewis acid base complexes $\text{AsCl}(\text{N}_3)_2\cdot\text{pyridine}$ and $\text{SbCl}_2\text{N}_3\cdot 2\text{ pyridine}$ were prepared. The products formed were characterised by Raman, IR and NMR spectroscopy. Density functional theory (B3LYP) was applied to calculate structural and vibrational data. Vibrational assignments of the normal modes for the isolated compounds were made on the basis of their vibrational spectra in comparison with com-

putational results. The molecular structures of both complexes were determined by X-ray diffraction. The bonding situation of these Lewis acid base complexes is discussed on the basis of NBO analyses, which were performed, on the crystallographic data.

(© Wiley-VCH Verlag GmbH, 69451 Weinheim, Germany, 2002)

Introduction

Mixed halogen compounds of arsenic and antimony are known few in number. A compound does exist in the +5 oxidation state with the empirical formula AsCl_2F_3 , which has an ionic structure with the composition $[\text{AsCl}_4][\text{AsF}_6]$ in the solid state.^[1] This salt is a synthon for the preparation of chlorofluoroarsoranes. The mixed chlorofluoroarsorane AsCl_4F was synthesised by vacuum thermolysis of $[\text{AsCl}_4][\text{AsF}_6]$.^[2] AsCl_2F_3 ^[3] and AsClF_4 ^[4] were formed by intermolecular ligand exchange in the gas phase at 173 K. These compounds are extremely unstable due to dismutation under halogen exchange in the respective halides.^[5] AsCl_2F_3 is the only structurally characterised mixed halogen compound of arsenic. The gas-phase structure of AsCl_2F_3 has been determined experimentally by electron diffraction.^[5]

AsCl_2Br and AsClBr_2 are the only reported mixed halogen compounds of arsenic in the +3 oxidation state. Müller et al. reported on the vibrational spectroscopic investigations of these mixed bromochloroarsanes.^[6,7] The isolation of these compounds as pure substances was not possible due to fast dismutation into the respective trihalides.^[6,8]

Mixed halogen/azide compounds in the +3 oxidation state are only reported for phosphorus. Dillon et al. characterised PX_2N_3 and $\text{PX}(\text{N}_3)_2$ ($\text{X} = \text{Cl}, \text{Br}$) by ^{31}P NMR spectroscopy.^[9] The corresponding fluoro compound (PF_2N_3) could be synthesised by the reaction of PF_2X ($\text{X} = \text{I}, \text{Br}$) with MN_3 ($\text{M} = \text{Na}, \text{Li}$)^[10] or PF_2Cl with NaN_3 .^[11]

SbCl_4N_3 is the only ternary synthesised^[12] and structurally characterised antimony(v) azide species. X-ray diffraction revealed that this compound shows a dimeric structure in the solid state.^[13]

Recently, we reported on the first structurally characterised ternary halogen/azide compound of antimony, $\text{SbCl}(\text{N}_3)_2$.^[14] In this paper we report about the synthesis, the spectroscopic properties, the crystal structures and NBO (Natural Bond Orbital) analyses of the first mixed halide pseudohalide arsenic(III) species as its pyridine adduct, $\text{AsCl}(\text{N}_3)_2\cdot\text{pyridine}$, as well as the monoazido-substituted antimony(III) species as its pyridine adduct, $\text{SbCl}_2\text{N}_3\cdot 2\text{pyridine}$.

Results and Discussion

Syntheses and Properties

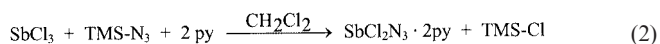
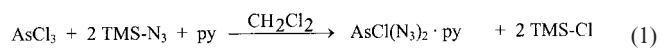
The synthesis and characterisation of mixed halogen azide compounds of arsenic and antimony in the +3 oxidation state proved to be very difficult. On the one hand the compounds tend to dismutate easily,^[6,8] on the other hand there is no suitable means of characterising such compounds. Neither the ^{75}As nor the ^{121}Sb nuclei can be detected by NMR spectroscopy in the +3 oxidation state due to the large quadrupole moment of these nuclei.^[15]

Reactions of MF_3 ($\text{M} = \text{As}, \text{Sb}$) with stoichiometric amounts of AgN_3 , NaN_3 or $\text{TMS}-\text{N}_3$ seemed to be especially suited for the synthesis of mixed halogen azide species of arsenic and antimony. These reactions were monitored by ^{14}N and ^{19}F NMR spectroscopy. It was shown, that in the ^{14}N NMR spectra resonances occurred, which could be assigned to covalently bound azide species. The ^{19}F NMR spectra, however, showed resonances, which could be assigned to AsF_3 and SbF_3 . It thus follows that intermediary formed mixed fluoride/azide species dismutate easily into the trifluorides and triazides, respectively.

[a] Department of Chemistry, Ludwig-Maximilians-Universität München, Butenandtstr. 5–13, 81377 München, Germany
Fax: (internat.) + 49-(0)89/2180-7492
E-mail: Thomas.M.Klapoetke@cup.uni-muenchen.de
[‡] X-ray structure determination

Raman spectroscopy also shows that the reactions of MX_3 ($\text{M} = \text{As}, \text{Sb}; \text{X} = \text{Br}, \text{I}$) with AgN_3 , NaN_3 or TMS-N_3 dismutate in the respective trihalides and triazides.

Reactions of arsenic(III) and antimony(III) chloride with TMS-N_3 yielded the expected compounds. Admittedly, the compounds could only be crystallised as Lewis acid base adducts with pyridine. The compounds were synthesised according to Equations (1) and (2).



NMR Properties

$\text{AsCl}(\text{N}_3)_2 \cdot \text{pyridine}$ and $\text{SbCl}_2\text{N}_3 \cdot 2\text{pyridine}$ have been characterised by ^1H , ^{13}C and ^{14}N NMR spectroscopy. The most useful method for the characterisation of covalently bonded azides is undoubtedly ^{14}N NMR spectroscopy. For covalently bound azide species three well-resolved resonances can be found in the ^{14}N NMR spectra and assignment of the individual resonances to N_α , N_β and N_γ (connectivity: $\text{M}-\text{N}_\alpha-\text{N}_\beta-\text{N}_\gamma$) was made on the basis of arguments given in the literature.^[16–18] The N_β atom of $\text{AsCl}(\text{N}_3)_2 \cdot \text{pyridine}$ shows a very sharp resonance at $\delta = -139$ ppm, the N_γ atom at $\delta = -181$ ppm and the N_α atom a very broad resonance at $\delta = -269$ ppm; $\text{SbCl}_2\text{N}_3 \cdot 2\text{pyridine}$ shows the analogous resonances at $\delta = -143$ (N_β), -172 (N_γ) and -275 ppm (N_α). In addition to these resonances, the spectra show resonances at $\delta = -164$ ppm [$\text{AsCl}(\text{N}_3)_2 \cdot \text{pyridine}$] and $\delta = -157$ ppm ($\text{SbCl}_2\text{N}_3 \cdot 2\text{pyridine}$). These resonances can be assigned to the nitrogen atoms of the pyridine rings. The resonances are shifted significantly towards higher field compared to free pyridine (pyridine: $\delta = -64$ ppm).^[19] Not only do the com-

pounds form stable adducts in the solid state but also in solution. The ^1H and ^{13}C NMR spectra show the expected resonances for pyridine (see Exp. Sect.).

Vibrational Spectra

Table 1 summarises selected computed and experimentally observed IR and Raman frequencies for $\text{AsCl}(\text{N}_3)_2 \cdot \text{pyridine}$ and $\text{SbCl}_2\text{N}_3 \cdot 2\text{pyridine}$. The recorded vibrational data agree well enough with our theoretical calculations (B3LYP) to allow assignment. It should be kept in mind that the computations were carried out for single, isolated (gas-phase) molecules. There may well be significant differences between gas-phase and solid-state spectra.

The measured IR and Raman spectra clearly show the presence of azide ligands bonded covalently to arsenic or antimony, as demonstrated by the simultaneous appearance of the antisymmetric (ca. 2100 cm^{-1}) and the symmetric (1250 cm^{-1}) azide stretching mode in both spectra (IR and Raman) and the presence of strong As–N and Sb–N stretching bands at ca. 386 cm^{-1} up to 452 cm^{-1} again in the IR and the Raman spectra. Based on our calculations the deformation vibration of the azide group should be split into four signals due to “in phase” and “out of phase” coupling of the “in plane” ($637\text{--}670 \text{ cm}^{-1}$) and “out of plane” ($567\text{--}595 \text{ cm}^{-1}$) deformation. The δN_3 “in phase” vibration appears at higher frequencies compared to the δN_3 “out of phase” vibration.

The symmetric Sb–Cl stretching vibration of $\text{SbCl}_2\text{N}_3 \cdot 2\text{pyridine}$ shows a signal at 326 cm^{-1} in the Raman spectrum and the antisymmetric stretching vibration shows a signal at 285 cm^{-1} . Both vibration modes are therefore shifted significantly to lower frequencies compared to the symmetric and antisymmetric Sb–Cl stretching modes of the parent SbCl_3 (ν_{as} : Sb–Cl 381 cm^{-1} ; ν_{s} : Sb–Cl 359 cm^{-1}).^[20] The Sb–Cl stretching modes of $\text{SbCl}(\text{N}_3)_2$ appear at 347 cm^{-1} .^[14] These signals are less shifted towards

Table 1. Selected calculated (B3LYP) and observed vibrational frequencies [cm^{-1}] for $\text{AsCl}(\text{N}_3)_2 \cdot \text{pyridine}$ and $\text{SbCl}_2\text{N}_3 \cdot 2\text{pyridine}$

$\text{AsCl}(\text{N}_3)_2 \cdot \text{pyridine}$			$\text{SbCl}_2\text{N}_3 \cdot 2\text{pyridine}$			Assignment
calcd. ^{[a][b]}	Raman ^[c]	IR	calcd. ^{[a][b]}	Raman ^[c]	IR	
2267 (500)	2118 (2.5)	2113 vs	2254 (646)	2091 (0.5)	2136 m	$\nu_{\text{as}}\text{N}_3$ “in phase” ^[d]
2244 (506)	2085 (1.5)				2079 vs	$\nu_{\text{as}}\text{N}_3$ “out of phase” ^[d]
1327 (146)	1268 (1)		1343 (153)	1210 (2)	1251 s	$\nu_{\text{s}}\text{N}_3$ “in phase” ^[d]
1312 (174)	1258 (0.5)	1257 vs				$\nu_{\text{s}}\text{N}_3$ “out of phase” ^[d]
662 (20)	670 (1.5)	670 sh	658 (10)	650 (1.5)	648 w	δN_3 “in phase” ^[d]
651 (17)	647 (1)	637 s				δN_3 “out of phase” ^[d]
585 (11)			595 (11)		594 s	δN_3 “in phase/90°” ^[d]
581 (7)		567 m				δN_3 “out of phase/90°” ^[d]
444 (25)	452 (10)		404 (28)	386 (2)		$\nu_{\text{s}}\text{MN}_{\text{azide}}$ ^[e]
407 (89)	433 (1)	431 m				$\nu_{\text{as}}\text{MN}_{\text{azide}}$ ^[e]
275 (15)	265 (2.5)		238 (13)	241 (4)		$\delta\text{MN}_{\text{azide}}$
321 (173)	287 (2)		306 (109)	326 (10)		$\nu_{\text{s}}\text{MCl}$
			293 (135)	285 (9)		$\nu_{\text{as}}\text{MCl}$
232 (9)	216 (2)		157 (9)	166 (1.5)		$\nu\text{MN}_{\text{pyridine}}$
135 (1)	139 (1.5)		108 (1)	108 (3)		$\delta\text{MN}_{\text{pyridine}}$

^[a] In parentheses: IR intensity [in km mol^{-1}]. ^[b] In parentheses: rel. Raman intensity. ^[c] The distinction “in/out of phase” is not applicable for $\text{SbCl}_2\text{N}_3 \cdot 2\text{pyridine}$. ^[d] The distinction “symmetric/antisymmetric” is not applicable for $\text{SbCl}_2\text{N}_3 \cdot 2\text{pyridine}$. ^[e] All calculated frequencies are unscaled.

lower frequencies. Therefore, the Sb–Cl bond lengths should decrease in the following order: $\text{SbCl}_2\text{N}_3 \cdot 2\text{pyridine} > \text{SbCl}(\text{N}_3)_2 > \text{SbCl}_3$. Increasing Sb–Cl bond lengths should cause decreasing Sb–Cl stretching modes towards lower frequencies. A similar shift of the As–Cl stretching mode could be observed for $\text{AsCl}(\text{N}_3)_2 \cdot \text{pyridine}$ in the Raman spectrum. The As–Cl stretching mode shows a band at 287 cm^{-1} and is therefore significantly shifted to lower frequencies, by about 120 cm^{-1} , compared to the symmetric and antisymmetric As–Cl stretching modes of the parent AsCl_3 .^[20] For this, the As–Cl bond lengths should be longer compared with the parent, AsCl_3 . This presumption could be verified by X-ray determination in both cases [see crystal structure of $\text{AsCl}(\text{N}_3)_2 \cdot \text{pyridine}$].

The covalent donor–acceptor properties of $\text{AsCl}(\text{N}_3)_2 \cdot \text{pyridine}$ and $\text{SbCl}_2\text{N}_3 \cdot 2\text{pyridine}$ can be obtained by signals assigned to the As– and Sb– N_{py} stretching and deformation vibrations. $\text{AsCl}(\text{N}_3)_2 \cdot \text{pyridine}$ shows a band at 216 cm^{-1} assigned to the As– N_{py} stretching mode. The deformation mode appears at 139 cm^{-1} ; $\text{SbCl}_2\text{N}_3 \cdot 2\text{pyridine}$ shows the analogous stretching mode at 166 cm^{-1} and the analogous deformation mode at 108 cm^{-1} in the Raman spectrum.

Crystal Structure of $\text{AsCl}(\text{N}_3)_2 \cdot \text{pyridine}$

$\text{AsCl}(\text{N}_3)_2 \cdot \text{pyridine}$ crystallises in the triclinic space group $P\bar{1}$ with two molecules in the unit cell (Figure 1). The crystallographic data and refinement details for this compound are summarised in the Exp. Sect. The experimentally observed and calculated bond lengths and bond angles are compiled in Table 2.

The arsenic atom is surrounded in a ψ -trigonal-bipyramidal fashion by three nitrogen atoms and one chlorine atom. Both azide ligands ($\text{N}2-\text{N}3-\text{N}4$ and $\text{N}5-\text{N}6-\text{N}7$) are in an equatorial position. The axial positions are occupied by the coordinating pyridine molecule and the chlorine atom. The free lone pair of the arsenic atom occupies, in accordance with the predictions of the VSEPR model,^[21] the third equatorial position, due to the fact that the lone pair re-

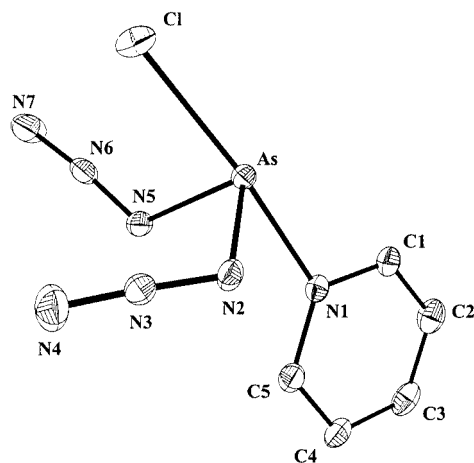


Figure 1. Molecular structure of $\text{AsCl}(\text{N}_3)_2 \cdot \text{pyridine}$ (hydrogen atoms are omitted for clarity); the thermal ellipsoids represent a 25% probability

Table 2. Selected calculated (B3LYP) and observed bond lengths [Å] and bond angles [°] for $\text{AsCl}(\text{N}_3)_2 \cdot \text{pyridine}$

	X-ray determination	B3LYP calculation
As–N(1)	2.158(3)	2.459
As–Cl	2.4848(9)	2.296
As–N(2)	1.897(2)	1.914
As–N(5)	1.916(3)	1.914
N(2)–N(3)	1.210(4)	1.235
N(3)–N(4)	1.138(4)	1.140
N(5)–N(6)	1.185(4)	1.235
N(6)–N(7)	1.149(4)	1.140
N(1)–As–N(2)	84.1(1)	79.9
N(1)–As–N(5)	85.9(1)	79.9
Cl–As–N(2)	91.35(8)	97.2
Cl–As–N(5)	91.56(9)	97.2
N(2)–As–N(5)	94.9(1)	99.8
Cl–As–N(1)	174.51(6)	175.4
As–N(2)–N(3)	117.6(2)	119.7
As–N(5)–N(6)	118.0(2)	119.7
N(2)–N(3)–N(4)	175.7(3)	175.0
N(5)–N(6)–N(7)	174.2(3)	175.0

quires more space compared to the pyridine molecule and the chlorine atom. The experimentally observed and calculated (B3LYP) bonding parameters agree with this predicted ψ -trigonal-bipyramidal arrangement of the ligands (Table 2).

The molecule does not show any special symmetry within the crystal. The calculations at the B3LYP level of theory predict an ideal C_s symmetry for this molecule in the gas phase. The predicted mirror plane can also almost be found in the crystal structure. The shape of this molecule agrees very well with the shape of the Lewis acid base adduct $\text{AsCl}_3 \cdot \text{NMe}_3$.^[22]

The calculated bonding parameters of the azide ligands are in good agreement with the experimentally observed As–N and N–N bond lengths as well as with the As–N–N and N–N–N bond angles (Table 2). The molecule shows a relatively long bond between the arsenic and chlorine atom [2.4848(9) Å], whereas the coordinative bond between the arsenic atom and the nitrogen molecule of the pyridine ring is very short [As–N1 2.158(3) Å]. The strong coordination of the very strong Lewis base pyridine at the arsenic centre weakens the As–Cl bond. This lengthens the As–Cl bond, which is significantly longer than it is in the cationic species AsCl_4^+ [2.042(3)–2.0545(9) Å]^[1,23] or binary AsCl_3 [2.17(2) Å].^[24]

The calculations show a coordinative bond (2.459 Å) between the arsenic atom and the nitrogen atom of the pyridine ring, which is weaker in the gas phase compared to the solid state [2.158(3) Å]. Due to the weaker interaction between the Lewis acid $\text{AsCl}(\text{N}_3)_2$ and the Lewis base in the gas phase, the calculated As–Cl bond shows a normal bond length (2.296 Å).

It should be noted, that structures of such weakly bound systems may differ considerably between the gas phase and the solid state.^[25,26]

$\text{SbCl}_2\text{N}_3 \cdot 2\text{pyridine}$ crystallises in the orthorhombic space group $Pbca$ with eight molecules in the unit cell and the lattice parameters $a = 6.5566(5)$, $b = 13.635(1)$ and $c = 30.901(2)$ (Figure 2). The experimentally observed and calculated (B3LYP) bond parameters are summarized in Table 3.

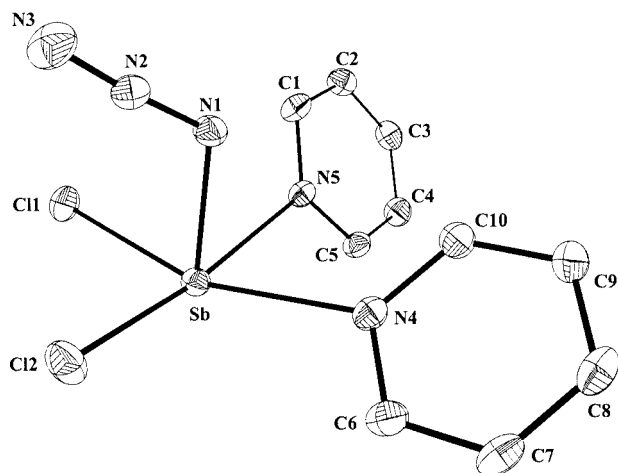


Figure 2. Molecular structure of $\text{SbCl}_2\text{N}_3 \cdot 2\text{pyridine}$ (hydrogen atoms are omitted for clarity); the thermal ellipsoids represent a 25% probability

Table 3. Selected calculated (B3LYP) and observed bond lengths [\AA] and bond angles [$^\circ$] for $\text{SbCl}_2\text{N}_3 \cdot 2\text{pyridine}$

	X-ray determination	B3LYP calculation
Sb–N(1)	2.084(2)	2.101
Sb–Cl(1)	2.4995(8)	2.451
Sb–Cl(2)	2.5352(8)	2.461
Sb–N(4)	2.466(2)	2.790
Sb–N(5)	2.392(2)	2.687
N(1)–N(2)	1.210(3)	1.230
N(2)–N(3)	1.141(3)	1.143
N(1)–Sb–Cl(1)	86.40(7)	93.1
N(1)–Sb–Cl(2)	87.91(7)	95.1
Cl(1)–Sb–Cl(2)	95.96(3)	95.0
N(1)–Sb–N(4)	78.14(9)	77.6
N(1)–Sb–N(5)	78.30(8)	75.2
N(4)–Sb–N(5)	82.24(8)	95.4
N(4)–Sb–Cl(1)	162.90(6)	170.2
N(5)–Sb–Cl(2)	165.55(6)	170.2
Sb–N(1)–N(2)	119.1(2)	120.1
N(1)–N(2)–N(3)	175.9(3)	175.3

The crystal structure reveals that $\text{SbCl}_2\text{N}_3 \cdot 2\text{pyridine}$ forms isolated molecules without intermolecular contacts, in which the antimony atom is surrounded, in an Ψ -octahedral or square-pyramidal fashion by three nitrogen atoms, two chlorine atoms and a free lone pair. The pyridine molecules and the chlorine atoms occupy the edges of an almost ideal planar plane. The N1 atom of the azide ligand occupies the top of the square pyramid. The experimentally observed and calculated bond parameters prove

that the arrangement of the ligands is Ψ -octahedral (ca. 90° , Table 3).

The structural parameters obtained for the azide unit compares well with the calculated parameters. The Sb–N1 bond that is 2.084(2) \AA , along with the N–N bond lengths within the azide unit, are in agreement with Sb–N and N–N bond lengths of other antimony azide compounds.^[13,27–30]

The average Sb–Cl bond lengths are 2.5174 \AA . Compared to the Sb–Cl bond lengths of SbCl_3 (2.36 \AA)^[31] these bond lengths are noticeably longer. Similar Sb–Cl bond lengths could only be observed in the bridging $\text{Sb}_2\text{Cl}_8^{2-}$ anions^[32,33] or the Lewis acid base adduct $\text{SbCl}_3 \cdot \text{NH}_2\text{Ph}$ ^[34] (2.52 \AA).

The average Sb–N bond lengths between the antimony atom and the nitrogen atom of the coordinating pyridine molecule are 2.429 \AA , leading to a relatively weak coordination of the pyridine molecules.

NBO Analyses

The molecular adduct complexes of arsenic and antimony trihalides or pseudohalides with pyridine are typical Lewis acid–base complexes. One of the major characteristics of these adducts is the total charge transfer q_{ct} between the donor molecule (pyridine) and the acceptor molecules [$\text{AsCl}(\text{N}_3)_2$ and SbCl_2N_3]. To obtain further insight into the donor–acceptor interaction we carried out NBO analyses on the data of the crystal structures of the two complexes.^[35,36]

The NBO analyses of the adduct complexes $\text{AsCl}(\text{N}_3)_2 \cdot \text{pyridine}$ and $\text{SbCl}_2\text{N}_3 \cdot 2\text{pyridine}$ show fairly polarised molecules. Table 4 summarises the NPA (Natural Population Analysis) partial charges and the total amount of transferred charge in both adducts.

Table 4. NPA partial charges (e) for $\text{AsCl}(\text{N}_3)_2 \cdot \text{pyridine}$ and $\text{SbCl}_2\text{N}_3 \cdot 2\text{pyridine}$

	$\text{AsCl}(\text{N}_3)_2 \cdot \text{pyridine}$	$\text{SbCl}_2\text{N}_3 \cdot 2 \text{pyridine}$
M (M = As, Sb)	1.35	1.46
Cl ^[a]	−0.55	−0.56
N _{py} ^[b]	−0.53	−0.53
N _a ^[c]	−0.68	−0.75
N _b ^[c]	0.24	0.24
N _c ^[c]	−0.07	−0.09
q_{ct}	0.20	0.27

^[a] Average of two chlorine atoms in $\text{SbCl}_2\text{N}_3 \cdot 2\text{pyridine}$. ^[b] Average of two nitrogen atoms of the pyridine rings in $\text{SbCl}_2\text{N}_3 \cdot 2\text{pyridine}$.

^[c] Average of the equivalent azide nitrogen atoms in $\text{AsCl}(\text{N}_3)_2 \cdot \text{pyridine}$.

The total amount for the charge transfer q_{ct} in these donor–acceptor complexes from the pyridine molecules to the Lewis acids $[\text{AsCl}(\text{N}_3)_2]$ and $[\text{SbCl}_2\text{N}_3]$ was found to be 0.20 electrons for $\text{AsCl}(\text{N}_3)_2\cdot\text{pyridine}$ and 0.27 electrons for $\text{SbCl}_2\text{N}_3\cdot 2\text{pyridine}$. This result is in good agreement with the concept of +I and –I effects.

In $\text{SbCl}_2\text{N}_3\cdot 2\text{pyridine}$ 0.13 electrons are transferred from one pyridine molecule and 0.14 electrons are transferred from the other pyridine molecule to the antimony centre. Therefore, the donor–acceptor interaction of $\text{SbCl}_2\text{N}_3\cdot 2\text{pyridine}$ is much weaker than in $\text{AsCl}(\text{N}_3)_2\cdot\text{pyridine}$. This is in good agreement with the experimentally obtained $\text{As}-\text{N}_{\text{py}}$ and $\text{Sb}-\text{N}_{\text{py}}$ bond lengths. The $\text{As}-\text{N}_{\text{py}}$ bond is extremely short [2.158(3) Å] and leads to a very strong interaction between the pyridine molecule and the $\text{AsCl}(\text{N}_3)_2$ unit. The average $\text{Sb}-\text{N}_{\text{py}}$ bond lengths are noticeably longer (2.429 Å), pointing to a weaker interaction.

In addition, the NBO analyses at the B3LYP level of theory show that within the azide units, the charge distribution is fairly polarised. The N_α atoms of the azide unit have an average charge of –0.72 electron, the N_β atoms have an average charge of +0.24 electrons and the terminal N_γ atoms 0.08 electrons (connectivity: $\text{M}-\text{N}_\alpha-\text{N}_\beta-\text{N}_\gamma$).

Conclusion

Mixed chloride/azide compounds of arsenic and antimony in the +3 oxidation state could be synthesised. $\text{AsCl}(\text{N}_3)_2$ and SbCl_2N_3 were crystallised as pyridine adducts.

These adducts were characterised by Raman, IR and multinuclear NMR spectroscopy. The structures and normal modes were calculated at the B3LYP level of theory, and compared with experimentally observed data. The agreement between theory and experiment is good. The vibrational spectra of $\text{AsCl}(\text{N}_3)_2\cdot\text{pyridine}$ and $\text{SbCl}_2\text{N}_3\cdot 2\text{pyridine}$ show bands, which can be assigned to the stretching vibrations as well as the deformation vibrations of the $\text{M}-\text{N}_{\text{py}}$ bonds ($\text{M} = \text{As}, \text{Sb}$).

Both adducts have been characterised by ^{14}N NMR spectroscopy. The ^{14}N NMR spectra show, in addition to three signals which can be assigned to the three different nitrogen atoms of the azide units, signals which can be assigned to the nitrogen atoms of the coordinated pyridine molecules. These resonances are significantly shifted compared to free pyridine.

Adduct structures which represent true minima structures ($\text{NIMAG} = 0$) were found for both adducts. The agreement between the calculated and experimentally observed bonding parameters is exceedingly good. The central atoms in $\text{AsCl}(\text{N}_3)_2\cdot\text{pyridine}$ are surrounded in a Ψ -trigonal-bipyramidal fashion, those in $\text{SbCl}_2\text{N}_3\cdot 2\text{pyridine}$ are Ψ -octahedral.

On the basis of the experimentally observed atom coordinates, NBO analyses (B3LYP) have been performed to ob-

tain more insight into the bonding situation of those weakly bonded Lewis acid base adducts. In $\text{AsCl}(\text{N}_3)_2\cdot\text{pyridine}$ 0.20 electrons are transferred from the pyridine molecule to $\text{AsCl}(\text{N}_3)_2$ and in $\text{SbCl}_2\text{N}_3\cdot 2\text{pyridine}$ 0.27 electrons of both pyridine molecules are transferred to SbCl_2N_3 . The average interaction of each pyridine molecule is much weaker than that of $\text{AsCl}(\text{N}_3)_2\cdot\text{pyridine}$. This result is reflected in the experimentally observed $\text{M}-\text{N}_{\text{py}}$ bond lengths.

Experimental Section

General Remarks: **CAUTION:** Arsenic and antimony azide compounds are toxic and potentially explosive! They may explode violently under various conditions and should be handled only in small amounts with extreme care. The use of safety equipment like leather gloves, leather coat and face-shield is strongly recommended. AsCl_3 ^[37] was prepared by literature methods and freshly distilled prior to use. Commercially available SbCl_3 (Fluka) was sublimed twice prior to use. Pyridine (Aldrich) and $(\text{CH}_3)_3\text{SiN}_3$ (Aldrich) were used as received. CH_2Cl_2 was dried by standard methods and freshly distilled prior to use. All the compounds reported here are moisture sensitive. Consequently, all manipulations were carried out under dinitrogen using Schlenk-techniques. NMR: Jeol EX 400, ^1H (400.0 MHz), ^{13}C (100.0 MHz): chemical shifts refer to $\delta(\text{TMS}) = 0.00$ ppm; ^{14}N (28.6 MHz): shifts refer to CH_3NO_2 . IR: Nicolet 520 FT-IR (KBr pellets). Raman: Perkin–Elmer FTIR-2000 spectrometer (Nd-Yag Laser: 1064 nm).

[Arsenic(iii) Diazide-Chloride]–Pyridine: $(\text{CH}_3)_3\text{SiN}_3$ (0.53 mL, 4.0 mmol) was added to a solution of AsCl_3 (0.17 mL, 2.0 mmol) in 25 mL of CH_2Cl_2 at 25 °C. After 1 h of stirring at room temperature, pyridine (0.32 mL, 4.00 mmol) was added. The solvent and the resulting $(\text{CH}_3)_3\text{SiCl}$ were removed in a dynamic vacuum. After recrystallisation from CH_2Cl_2 at –25 °C, colourless crystals were obtained. Yield 0.39 g (71%). IR (KBr): $\tilde{\nu} = 3066$ (m), 2113 (vs, ν_{asN_3}), 1635 (w), 1600 (s), 1537 (s), 1486 (s), 1447 (vs), 1339 (m), 1257 (vs, ν_{sN_3}), 1158 (m), 1065 (s), 1036 (s), 1008 (s), 946 (m), 755 (s), 670 (sh, δN_3), 637 (s, δN_3), 567 (m, δN_3), 431 (m, ν_{asN}) cm^{-1} . Raman (66 scans, 150 mW, 180°, 20 °C): $\tilde{\nu} = 3073$ (3), 2118 (2.5, ν_{asN_3}), 2085 (1.5, ν_{asN_3}), 1606 (1), 1575 (1), 1268 (1, ν_{sN_3}), 1258 (0.5, ν_{sN_3}), 1038 (3), 1013 (4), 670 (1.5, δN_3), 647 (1, δN_3), 452 (10, ν_{asN}), 433 (1, ν_{asN}), 287 (2, ν_{asCl}), 265 (2.5, δasN), 216 (2, $\nu_{\text{asN}_{\text{py}}}$), 180 (3), 139 (1.5, $\delta\text{asN}_{\text{py}}$) cm^{-1} . ^1H NMR (CD_2Cl_2 , 25 °C): $\delta = 6.33$ (m, 2-H), 7.12 (m, 3-H), 8.22 (d, 1-H) ppm. ^{13}C NMR (CD_2Cl_2 , 25 °C): $\delta = 124.0$ (s, C-2), 127.7 (m, C-3), 141.1 (d, C-1) ppm. ^{14}N NMR (CH_2Cl_2 , 25 °C): $\delta = -139$ (s, N_β), –164 (s, N_{py}), –181 (s, N_γ), –269 (s, N_α) ppm.

[Antimony(iii) Azide Dichloride]–2Pyridine (2): $(\text{CH}_3)_3\text{SiN}_3$ (0.26 mL, 2.0 mmol) was added to a solution of SbCl_3 (0.456 g, 2.0 mmol) in 25 mL of CH_2Cl_2 at 25 °C. After 1 h of stirring at room temperature, pyridine (0.32 mL, 4.00 mmol) was added. The solvent and the resulting $(\text{CH}_3)_3\text{SiCl}$ were removed in a dynamic vacuum. After recrystallisation from CH_2Cl_2 at –25 °C, colourless crystals were obtained. Yield 0.52 g (66%). IR (KBr): $\tilde{\nu} = 3063$ (m), 2136 (m, ν_{asN_3}), 2079 (vs, ν_{asN_3}), 1634 (s), 1608 (s), 1538 (s), 1485 (s), 1389 (w), 1331 (m), 1251 (s, ν_{sN_3}), 1179 (s, 1054 (s), 1004 (s), 936 (m), 750 (s), 648 (w, δN_3), 594 (s, δN_3), 509 (m) cm^{-1} . Raman (196 scans, 150 mW, 180°, 20 °C): $\tilde{\nu} = 3075$ (3.5), 2091 (0.5,

ν_{AsN_3} , 1602 (2), 1572 (1.5), 1210 (2, ν_{SbN_3}), 1035 (5), 1014 (5), 650 (1.5, δ_{N_3}), 386 (2, ν_{SbN}), 326 (10, ν_{SbCl}), 285 (9, ν_{SbCl}), 241 (4, δ_{SbN}), 166 (1.5, $\nu_{\text{SbN}_{\text{py}}}$), 108 (3, $\delta_{\text{SbN}_{\text{py}}}$) cm^{-1} . ^1H NMR (CD_2Cl_2 , 25 °C): δ = 6.52 (m, 2-H), 7.42 (m, 3-H), 8.32 (d, 1-H) ppm. ^{13}C NMR (CD_2Cl_2 , 25 °C): δ = 124.9 (s, C-2), 126.7 (m, C-3), 143.2 (d, C-1) ppm. ^{14}N NMR (CH_2Cl_2 , 25 °C): δ = -143 (s, N_{β}), -157 (s, N_{py}), -172 (s, N_{γ}), -275 (s, N_{α}) ppm.

X-ray Crystallographic Study: $\text{AsCl}(\text{N}_3)_2\cdot\text{pyridine}$: $\text{C}_5\text{H}_5\text{AsClN}_7$, M = 273.53, crystal size: $0.30 \times 0.30 \times 0.30$ mm, colourless prism, triclinic, space group $P\bar{1}$, a = 7.3826(8), b = 8.0314(9), c = 9.621(1) Å, α = 108.497(2), β = 103.881(2), γ = 101.632(2)°, V = 500.22(9) Å³, Z = 2, $d_{\text{calcd.}}$ = 1.816 Mg/m^3 , μ = 3.637 mm^{-1} , $F(000)$ = 268. Siemens SMART Area detector, Mo- K_{α} , λ = 0.71073 Å, T = 193(2) K, θ range = 2.36–28.73° in $-9 \leq h \leq 8$, $-10 \leq k \leq 10$, $-11 \leq l \leq 10$, reflections collected: 2847, independent reflections: 1494 (R_{int} = 0.0171), observed reflections: 1376 [$F > 4\sigma(F)$]. Structure solution program: SHELXS-97,^[38] full-matrix least-squares methods, parameter/restraints ratio: 127:0, final R indices [$F > 4\sigma(F)$]: R_1 = 0.0248, wR_1 = 0.0652; R_2 = 0.0278, wR_2 = 0.0668 (all data), GOF on F^2 = 1.042, largest difference peak/hole: 0.493/−0.419 $\text{e} \text{ Å}^{-3}$, program used: SHELXL-97.^[39] $\text{SbCl}_2\text{N}_3\cdot 2\text{pyridine}$: $\text{C}_{10}\text{H}_{10}\text{Cl}_2\text{N}_5\text{Sb}$, M = 392.88, crystal size: $0.30 \times 0.30 \times 0.30$ mm, colourless prism, orthorhombic, space group $Pbca$, a = 6.5566(5), b = 13.635(1), c = 30.901(2) Å, V = 2762.4(4) Å³, Z = 8, $d_{\text{calcd.}}$ = 1.889 Mg/m^3 , μ = 2.373 mm^{-1} , $F(000)$ = 1520. Siemens SMART Area detector, Mo- K_{α} , λ = 0.71073 Å, T = 193(2) K, θ range = 2.64–29.07° in $-8 \leq h \leq 8$, $-17 \leq k \leq 17$, $-30 \leq l \leq 41$, reflections collected: 14636, independent reflections: 2796 (R_{int} = 0.0285), observed reflections: 2369 [$F > 4\sigma(F)$]. Structure solution program: SHELXS-97,^[38] full-matrix least-squares methods, parameter/restraints ratio: 163:0, final R indices [$F > 4\sigma(F)$]: R_1 = 0.0243, wR_1 = 0.0530; R_2 = 0.0326, wR_2 = 0.0551 (all data), GOF on F^2 = 1.116, largest difference peak/hole: 0.267/−0.494 $\text{e} \text{ Å}^{-3}$, program used: SHELXL-97.^[39] CCDC-181324 and -181325 contain the supplementary crystallographic data for this paper. These data can be obtained free of charge at www.ccdc.cam.ac.uk/conts/retrieving.html or from the Cambridge Crystallographic Data Centre, 12, Union Road, Cambridge CB2 1EZ, UK [Fax: (internat.) + 44-1223/336-0333; E-mail: deposit@ccdc.cam.ac.uk].

Computational Methods: The structures and vibrational data for the reported compounds were calculated using the density functional theory with the program package Gaussian 98.^[40] The calculations were carried out at the electron-correlated B3LYP level of theory^[41] which includes a mixture of Hartree–Fock exchange with DFT exchange correlation. For C, H, N and Cl a standard 6-31G(d,p) double-zeta basis set was used and for As and Sb a quasi-relativistic pseudopotential (As: ECP28MWB; Sb: ECP46MWB)^[42] and a (5s5p1d)/[3s3p1d]-DZ+P basis set.^[43] Becke's 3-parameter functional, where the nonlocal correlation is provided by the LYP expression (Lee, Yang, Parr correlation functional), was used which is implemented in Gaussian 98.^[40]

Acknowledgments

We are indebted to and thank Dr. M.-J. Crawford for stimulating ideas to start this research. Financial support of this work by the University of Munich and the Fonds der Chemischen Industrie is gratefully acknowledged.

^[1] R. Minkwitz, J. Nowicki, *Z. Anorg. Allg. Chem.* **1991**, 596, 93.

^[2] R. Minkwitz, H. Prenzel, *Z. Anorg. Allg. Chem.* **1986**, 534, 150.

- ^[3] R. Minkwitz, F. Claus, M. Glaser, *Z. Anorg. Allg. Chem.* **1983**, 506, 178.
- ^[4] F. Claus, R. Minkwitz, *Z. Anorg. Allg. Chem.* **1983**, 501, 19.
- ^[5] R. Minkwitz, H. Prenzel, A. Schardey, H. Oberhammer, *Inorg. Chem.* **1987**, 26, 2730.
- ^[6] A. Müller, E. Niecke, B. Krebs, O. Glemser, *Z. Naturforsch., Teil B* **1968**, 23, 588.
- ^[7] A. Müller, B. Krebs, *J. Mol. Structure* **1968**, 2, 149.
- ^[8] H. Preiss, E. Alsdorf, A. Lehmann, *Carbon* **1987**, 25, 727.
- ^[9] K. B. Dillon, A. W. G. Platt, T. C. Waddington, *Inorg. Nucl. Chem. Lett.* **1978**, 14, 511.
- ^[10] E. L. Lines, L. F. Centofanti, *Inorg. Chem.* **1972**, 11, 2269.
- ^[11] S. R. O'Neill, J. M. Shreeve, *Inorg. Chem.* **1972**, 11, 1630.
- ^[12] ^[12a] U. Müller, K. Dehnicke, *Z. Anorg. Allg. Chem.* **1967**, 350, 113. ^[12b] A. Schmidt, *Chem. Ber.* **1971**, 104, 31.
- ^[13] U. Müller, *Z. Anorg. Allg. Chem.* **1972**, 388, 207.
- ^[14] T. M. Klapötke, H. Nöth, T. Schütt, M. Warchold, *Z. Anorg. Allg. Chem.* **2001**, 627, 81.
- ^[15] ^[15a] G. Baliman, P. S. Pregosin, *J. Magn. Reson.* **1977**, 26, 283. ^[15b] C. Brevard, P. Granger, *Handbook of High Resolution Multinuclear NMR*, J. Wiley, New York, Chichester, **1981**, p. 136–137. ^[15c] H. P. A. Mercier, J. C. P. Sanders, G. J. Schrobilgen, *J. Am. Chem. Soc.* **1994**, 116, 2921. ^[15d] M. F. A. Dove, J. C. P. Sanders, E. L. Jones, M. J. Parkin, *J. Chem. Soc., Chem. Commun.* **1984**, 1578.
- ^[16] T. M. Klapötke, H. Nöth, T. Schütt, M. Warchold, *Angew. Chem.* **2000**, 112, 2197; *Angew. Chem. Int. Ed.* **2000**, 39, 2108.
- ^[17] W. Beck, W. Becker, K. F. Chew, W. Derbyshire, N. Logan, D. M. Revitt, D. B. Sowerby, *J. Chem. Soc., Dalton Trans.* **1972**, 245.
- ^[18] M. Witanowski, *J. Am. Chem. Soc.* **1968**, 90, 5683.
- ^[19] G. A. Webb, *Annual Reports on NMR Spectroscopy*, Academic Press, Inc., London, **1986**, vol. 18.
- ^[20] K. Nakamoto, *Infrared and Raman Spectra of Inorganic and Coordination Compounds*, J. Wiley, New York, **1986**.
- ^[21] ^[21a] R. J. Gillespie, *Molecular Geometry*, Van Nostrand Reinhold, London, **1972**. ^[21b] R. J. Gillespie, I. Hargittai, *The VSEPR Model of Molecular Geometry*, Prentice-Hall, New Jersey, **1991**. ^[21c] R. J. Gillespie, *Chem. Soc. Rev.* **1991**, 21, 59.
- ^[22] M. Webster, S. Keats, *J. Chem. Soc. A* **1971**, 837.
- ^[23] M. Gerken, P. Kolb, A. Wegner, H. P. A. Mercier, H. Borrmann, D. A. Dixon, G. J. Schrobilgen, *Inorg. Chem.* **2000**, 39, 2813.
- ^[24] P. W. Allen, L. E. Sutton, *Acta Crystallogr.* **1950**, 3, 46.
- ^[25] R. Jürgens, J. Almöf, *Chem. Phys. Lett.* **1991**, 276, 263.
- ^[26] R. Ahlrichs, M. R. Bär, M. Häser, E. Sattler, *Chem. Phys. Lett.* **1991**, 184, 353.
- ^[27] D. F. Moser, I. Schranz, M. C. Gerrety, L. Stahl, R. J. Staples, *J. Chem. Soc., Dalton Trans.* **1999**, 751.
- ^[28] G. Ferguson, F. C. March, D. R. Ridley, *Acta Crystallogr., Sect. B* **1975**, 31, 1260.
- ^[29] J. Müller, U. Müller, A. Loss, J. Lorberth, H. Donath, W. Massa, *Z. Naturforsch., Teil B* **1985**, 40, 1320.
- ^[30] G. Ferguson, D. R. Ridley, *Acta Crystallogr., Sect. B* **1973**, 29, 2221.
- ^[31] N. N. Greenwood, A. Earnshaw, *Chemie der Elemente*, VCH, Weinheim, **1988**.
- ^[32] ^[32a] W. S. Sheldrick, H.-J. Häusler, J. Kaub, *Z. Naturforsch., Teil B* **1988**, 43, 789. ^[32b] A. T. Mohammed, U. Müller, *Acta Crystallogr., Sect. C* **1985**, 41, 329. ^[32c] W. Czado, S. Rabe, U. Müller, *Z. Naturforsch., Teil B* **1998**, 54, 288.
- ^[33] U. Ensinger, W. Schwarz, A. Schmidt, *Z. Naturforsch., Teil B* **1982**, 37, 1584.
- ^[34] R. Hulme, J. C. Scruton, *J. Chem. Soc. A* **1968**, 2448.
- ^[35] A. E. Reed, L. A. Curtiss, F. Weinhold, *Chem. Rev.* **1988**, 88, 899.

- [36] A. E. Reed, R. B. Weinstock, F. Weinhold, *J. Chem. Phys.* **1985**, *83*, 735.
- [37] G. Brauer, *Handbuch der präparativen anorganischen Chemie*, 2nd ed., F. Enke, Stuttgart, **1975**.
- [38] G. M. Sheldrick, *SHELXS-97, Program for Crystal Structure Solution*, Universität Göttingen, **1997**.
- [39] G. M. Sheldrick, *SHELXL-97, Program for Crystal Structure Refinement*, Universität Göttingen, **1997**.
- [40] M. J. Frisch, G. W. Trucks, H. B. Schlegel, G. E. Scuseria, M. A. Robb, J. R. Cheeseman, V. G. Zakrzewski, J. A. Montgomery, R. E. Stratmann, J. C. Burant, S. Dapprich, J. M. Millam, A. D. Daniels, K. N. Kudin, M. C. Strain, O. Farkas, J. Tomasi, V. Barone, M. Cossi, R. Cammi, B. Mennucci, C. Pomelli, C. Adamo, S. Clifford, J. Ochterski, G. A. Petersson, P. Y. Ayala, Q. Cui, K. Morokuma, D. K. Malick, A. D. Rabuck, K. Raghavachari, J. B. Foresman, J. Cioslowski, J. V. Ortiz, B. B. Stefanov, G. Liu, A. Liashenko, P. Piskorz, I. Komaromi, R. Gomperts, R. L. Martin, D. J. Fox, T. Keith, M. A. Al-Laham, C. Y. Peng, A. Nanayakkara, C. Gonzalez, M. Challacombe, P. M. W. Gill, B. Johnson, W. Chen, M. W. Wong, J. L. Andres, C. Gonzalez, M. Head-Gordon, E. S. Replogle, J. A. Pople, *Gaussian 98*, revision A.3, Gaussian, Inc., Pittsburgh PA, **1998**.
- [41] [41a] C. Lee, W. Yang, R. G. Parr, *Phys. Rev.* **1988**, *B37*, 785. [41b] A. D. Becke, *Phys. Rev.* **1988**, *A38*, 3098. [41c] B. Miehlich, A. Savin, H. Stoll, H. Preuss, *Chem. Phys. Lett.* **1989**, *157*, 200. [41d] A. D. Becke, *J. Chem. Phys.* **1993**, *98*, 5648.
- [42] A. Bergner, M. Dolg, W. Kuechle, H. Preuss, *Mol. Phys.* **1993**, *80*, 1431.
- [43] M. Kaupp, R. v. R. Schleyer, H. Stoll, H. Preuss, *J. Am. Chem. Soc.* **1991**, *113*, 1602.

Received March 15, 2002
[I02130]